Available online at www.sciencedirect.com
SCIENCE DIRECT®
Journal of Inorganic Biochemistry 99 (2005) 1135–1144
Journal of Inorganic Biochemistry
www.elsevier.com/locate/jinorgbio

C-MALISA (cellular magnetic-linked immunosorbent assay), a new application of cellular ELISA for MRI ☆

Carmen Burtea, Sophie Laurent, Alain Roch, Luce Vander Elst, Robert N. Muller *

Department of Organic and Biomedical Chemistry, NMR and Molecular Imaging Laboratory, University of Mons-Hainaut, 24, Avenue du Champ de Mars, B-7000 Mons, Belgium

Received 27 December 2004; received in revised form 7 February 2005; accepted 10 February 2005
Available online 9 March 2005

Abstract

A modified cellular ELISA (enzyme-linked immunosorbent assay), named cellular magnetic-linked immunosorbent assay (C-MALISA), has been developed as an application of magnetic resonance imaging (MRI) for in vitro clinical diagnosis. To validate the method, three contrast agents targeted to integrins were synthesized by grafting to USPIO (ultrasmall particles of iron oxide): (a) the CS1 (connecting segment-1) fragment of fibronectin (FN) (USPIO-g-FN); (b) the peptide GRGD (USPIO-g-GRGD); (c) a non-peptidic RGD mimetic (USPIO-g-mimRGD). Jurkat cells and rat mononuclear cells were stimulated to activate their integrins. After cell fixation on ELISA plates, incubation with the contrast agents, rinsing, and digestion in 5 N HCl, the samples were analyzed by MRI. Paramagnetic relaxation rate enhancements (ΔR_2) were measured on images. ΔR_2 was converted in values of iron concentration based on a calibration curve. The apparent dissociation constants (K_d^*) of the three contrast agents were estimated based on the MRI measurement of ΔR_2. K_d^* of 1.22×10^{-7} M, of 7.00×10^{-8} M, and of 1.13×10^{-8} M were found respectively for USPIO-g-FN, USPIO-g-GRGD, and USPIO-g-mimGRG. The MRI confirmed a statistically significant difference ($p < 0.01$, $p < 0.05$) between the stimulated cells incubated with integrin-targeted compounds with respect to the controls (i.e., non-stimulated cells and stimulated cells incubated with non-specific USPIO). The integrin specificity of the three compounds was confirmed by the pre-incubation with GRGD (for USPIO-g-mimRGD and USPIO-g-GRGD) or FN (for USPIO-g-FN).

Keywords: C-MALISA; Cellular ELISA; MRI; Magnetic nanoparticles; Integrins; Lymphocytes

1. Introduction

After its clinical introduction in the early 1980s, magnetic resonance imaging (MRI) became quickly one of the leading diagnostic techniques. The method is non-invasive and it yields real-time and real-volume images of the subject, either patient or tissues and molecular events. The use of contrast agents made the method even more sensitive and the diagnosis more accurate. The first generation of contrast agents was non-specific and reported solely on anatomy or allowed the evaluation of the physiological status of biological systems. Shortly after the first attempts to target specific tissues [1] or pathologies [2], a new generation of MR contrast agents has emerged and offered the opportunity to image gene expression, metabolic activity and neuronal activation [3,4]. A wide variety of vector and carrier molecules have been developed to deliver magnetic labels to specific target sites [5]. They were designed to target in vivo specific receptors and to report on a diversity of biological processes, which otherwise were accessible only in histologically stained and excised specimens. MRI thus became

☆ Parts of this work have been presented at the 20th Annual Meeting of ESMRMB Rotterdam, Netherlands, September 18–21, 2003.

* Corresponding author. Tel./Fax: +0032 65 373520.
E-mail address: Robert.Muller@umh.ac.be (R.N. Muller).

0162-0134/$ - see front matter © 2005 Elsevier Inc. All rights reserved.
doi:10.1016/j.jinorgbio.2005.02.009

an attractive tool both for clinical diagnosis and for biomedical research.

The potential of MRI contrast agents to image specific biochemical processes in vivo encounters several constraints, which are related to the minimal concentration of contrast agents able to exert a significant effect on the relaxation rate of tissue water and therefore on the MRI signal. Since cellular receptors are present in nano- or even picomolar concentrations, the contrast agents bound to these targets should exert an enormous magnetic effect in order to overcome the signal dilution in the relatively large voxels. This limitation can be solved by increasing the efficiency of contrast agents either by a greater intrinsic relaxivity or by the attachment of many magnetic centers to the ligand. Among the magnetic materials able to be detected at low tissue concentrations, one can point out the superparamagnetic particles [6], the paramagnetic dendrimers [7], and the perfluorocarbon nanoparticles [8]. In addition, the necessity to deliver contrast material in sufficient quantity at the targeted sites could lead to a possible saturation of cell receptors. This biochemical limitation was tentatively solved by targeting receptors involved in transport systems (e.g., receptor mediated endocytosis) or readily accessible to the vascular system [9].

The progress in hardware, contrast agents, and image acquisition methods assisted to the development of molecular imaging, a new medical discipline, which integrates cell biology, molecular biology and diagnostic imaging, bringing high expectations for MRI applications into drug discovery [10,11]. Molecular imaging has a wide diversity of applications, which range from the diagnosis of a particular pathology [12–18] to the monitoring of gene therapy or chemotherapy [19–22]. Cellular imaging is another growing field of interest both for medical research and for clinical application, which often appeals to iron oxide MR contrast agents [23] to image macrophage activity for diagnostic purposes [24,25] or to monitor the cell migration and trafficking [26].

A recent application of molecular imaging is related to the protocols of molecular biology and refers to the contrast agents as magnetic relaxation switches, capable of sensing biochemical interactions if the interacting molecules are magnetically labeled with iron oxide nanoparticles [27,28]. In fact, the molecular interactions result in a 30–40% change of the transverse relaxation time, T_2, which can be evaluated both by MR relaxometry or by MRI. Finally, MRI has been proposed as a high throughput screening modality for examining the interactions between superparamagnetic nanoparticles and cells [29].

In their work, Högemann et al. [29] have shown that MRI can accurately evaluate thousands of samples simultaneously and rapidly. Based on this observation, we have modified the cellular ELISA (enzyme-linked immunosorbent assay) technique with the purpose of developing an MRI application for clinical diagnosis, which was named cellular magnetic-linked immunosorbent assay (C-MALISA). In our protocol, the cells are fixed on ELISA plates, and their membrane receptors are detected and evaluated with specific contrast agents. As compared to classical ELISA, the ligand itself is labeled by a superparamagnetic moiety, which directly reports on the interaction with the specific receptor. The method offers the advantage of a real-time analysis of the ligand–receptor interaction, which is not the case with the classical methods of immunohistochemistry.

To validate the method, three contrast agents with affinity for the integrin family of adhesion molecules were synthesized by grafting to USPIO particles one of the following specific ligands: (a) the CS1 (connecting segment-1) fragment of fibronectin (USPIO-g-FN); (b) the peptide GRGD (USPIO-g-GRGD); (c) a non-peptide small molecular weight RGD mimetic (USPIO-g-mimRGD) [30]. The integrins are a ubiquitously expressed class of cell surface receptors involved in the cell–cell and cell–matrix interactions. These receptors represent an interesting therapeutic target because of their important role in diverse pathologies, i.e., restenosis, atherosclerosis, acute renal failure, and cancer [31]. The tripeptide sequence RGD (Arg-Gly-Asp) is a common cell-recognition motif, which is part of integrin binding ligands like fibronectin, fibrinogen, and vitronectin. The CS1 fragment of fibronectin contains the motif LDV (Leu-Asp-Val) which has high affinity for integrins $\alpha_4\beta_1$ (VLA-4, very late antigen-4) and $\alpha_4\beta_7$ [32].

In the present work, the affinity for integrins of the three contrast agents was tested by C-MALISA on Jurkat cells and on rat mononuclear cells (MNC), which were stimulated to activate their integrins. The cells were fixed on ELISA microtiter plates and analyzed by MRI after incubation with contrast agents. The concentration of bound contrast agents was estimated and their apparent constants of affinity for integrins were evaluated.

2. Materials and methods

2.1. Synthesis of USPIO-g-FN, USPIO-g-GRGD, and of USPIO-g-mimRGD

2.1.1. Synthesis of mimRGD

The RGD mimetic (mimRGD) (Fig. 1) was obtained as described by Sulyok et al. [30]. Synthesis was performed on solid support (trityl chloride polystyrol resin) by the Fmoc strategy. Briefly, reaction of 4-chlorobenzaldehyde with malonic acid resulted in the corresponding racemic β-aminoacid, which could be transformed into the Fmoc protected derivative with a high yield. These Fmoc protected carboxylic building blocks were attached to trityl chloride polystyrol resin (TCP) using

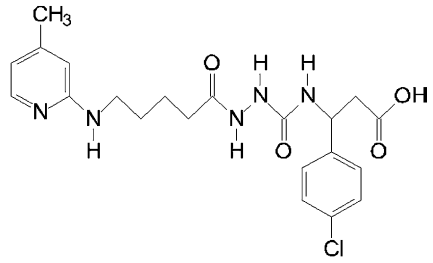

Fig. 1. Mimetic structure of the RGD sequence.

standard conditions [33]. *N*-Fmoc hydrazine was carbonylated with an excess of phosgene in toluene to obtain the activated azaglycine building block 5-(9H-Fluoren-9-ylmethoxy)-1,3,4-oxadiazol-2(3H)-one. After Fmoc deprotection the resin-bound β-amino acids were treated with an excess of oxadiazolone to yield the resin bound Fmoc protected azagly-β-amino acid derivatives. 2-amino-4-methylpyridine was treated with 5-bromopentanoic acid ethyl ester to give 5(4-methylpyridine-2-yl)aminopentanoic acid ethyl ester. After hydrolysis with NaOH, 5(4-methylpyridine-2-yl)aminopentanoic acid was obtained by precipitation. After deprotection of the resin bound Fmoc protected aza-compounds with piperidine, the derivative was coupled using the solid phase coupling conditions. The resulting resin bound aza RGD mimetic was deprotected and cleaved from the resin using trifluoroacetic acid.

2.1.2. Synthesis of USPIO-vectorized

The vectorizing groups were grafted on the magnetic nanoparticles by reaction with the dextran coating of USPIO previously treated with epichlorhydrin.

Five milliliters of USPIO (100 mg of Fe, dextran coated maghemite particles with a hydrodynamic size of 22 nm) obtained by coprecipitaion of Fe^{2+} and Fe^{3+} ions in basic medium is diluted in 25 mL of water and treated with 20 mL of NaOH 5 N and 10 mL of epichlorhydrin. The mixture is stirred for 24 h at 40 °C in the darkness and then dialyzed (cut-off of the membrane: 12,000–14,000; Spectra/Por, VWR, Leuven, Belgium) in a 5 mM sodium citrate buffer (pH 8).

A solution of GRGD (5 mg, Sigma, Bornem, Belgium), mimRGD (5 mg) or CS-1 fragment of fibronectin (10 mg, Bachem, Weil am Rhein, Germany) in 2 mL of water is added to the USPIO-epichlorhydrin suspension (90 μmol of Fe). The mixture is stirred at room temperature overnight and is exhaustively dialyzed to eliminate the free peptide or mimetic.

2.2. Characterization of USPIO-g-FN, USPIO-g-GRGD, and of USPIO-g-mimRGD

Iron concentration was determined by relaxometry at 20 MHz (Bruker Minispec PC-20, Bruker, Karlsruhe, Germany) and 37 °C after mineralization in acidic conditions (0.6 mL HNO_3 and 0.3 mL H_2O_2) by microwaves (Milestone MSL-1200, Sorisole, Italy).

Table 1
Relaxivities (s^{-1} mM Fe^{-1}) of USPIO-g-FN, USPIO-g-GRGD, and USPIO-g-mimRGD as compared to the parent compound USPIO measured in aqueous solutions at 1.5 T (60 MHz) and 37 °C

Compound	r_1 (s^{-1} mM^{-1})	r_2 (s^{-1} mM^{-1})	r_2/r_1
USPIO	11.3	63.1	5.7
USPIO-g-FN	11.3	76.0	6.7
USPIO-g-GRGD	11.2	84.9	7.6
USPIO-g-mimRGD	10.1	68.4	6.8

For USPIO-g-FN and USPIO-g-GRGD, the peptide concentration grafted to USPIO particles was determined by Bio-Rad protein assay (Bio-Rad Laboratories SA-NV, Nazareth, Belgium) and was found to be 3.77×10^{-4} mmol and 2.55×10^{-4} mmol per mmol of Fe, corresponding respectively to 4 and 2.8 molecules of peptide per particle by assuming an average of 11,000 iron atoms per particle. This number of iron atoms is a reasonable value if considering a particle mean diameter of about 8 nm, which is obtained by fitting the magnetic curve of our USPIO sample with a Langevin function. Since a unit cubic cell of magnetite has a size of 0.82 nm and contains 24 iron atoms, it is easy to calculate the average number of iron atoms in a spherical particle of 8 nm of diameter.

The compounds were characterized in vitro by relaxometry in aqueous solutions. Proton longitudinal (r_1) and transverse (r_2) relaxivities (Table 1) were measured at 60 MHz and 37 °C on a Bruker Minispec mq60 (Bruker, Karlsruhe, Germany).

2.3. Cell culture and stimulation of Jurkat cells

Jurkat cells (gift from Prof. Oberdan Leo, Free University of Brussels, IBMM, Belgium) were cultured at a concentration of 1×10^6/mL in RPMI 1640 medium (Sigma–Aldrich NV/SA, Bornem, Belgium) supplemented with 10% newborn calf serum and 1% antibiotic–antimicotic (both from Invitrogen NV/SA, Gibco, Merelbeke, Belgium). Cells were resuspended in fresh culture medium prior to exposure to 50 ng/mL phorbol 12-myristate 13-acetate (PMA, Sigma–Aldrich NV/SA, Bornem, Belgium) for 3 h [34]. The viability of cells was checked with trypan blue (Sigma–Aldrich NV/SA, Bornem, Belgium) before treatment and found to be larger than 90%. The cells were counted on a bright line counting chamber (Hausser Scientific, Sigma–Aldrich NV/SA, Bornem, Belgium) and the mean percentage of viable cells in three microscopic fields was calculated.

2.4. Stimulation and isolation of MNC

All the animal experiments fulfil the requirements of the Ethical Committee of our institution.

Wistar rats ($n = 4$/group, 269 ± 6 g, Harlan, Horst, The Netherlands) were anesthetized with i.p. injection of pentobarbital (Nembutal®, Sanofi Santé Animale, Brussels, Belgium) at a dose of 60 mg/kg b.w. Hepatitis was induced by i.v. injection of 20 mg/kg b.w. concanavalin A (ConA) [35]. Five hours later, the rats were tracheotomized and the left carotide was catheterized (Becton–Dickinson Angiocath 0.7×19 mm) for blood collection. The MNC were isolated by Histopaque density gradient (Sigma–Aldrich NV/SA, Bornem, Belgium) from the rat blood according to the supplier instructions.

2.5. The protocol of C-MALISA

The cells were suspended in 0.5% buffered formalin, pH 7.0, and fixed (2×10^6 cells/well) on ELISA microtiter plates (MICROLON® 600, Grenier Bio-One, Wemmel, Belgium) by drying for 24 h in airflow at 37 °C according to Walker et al. [36]. The ELISA plates were subsequently blocked for 2 h with 4% milk powder in phosphate buffered saline (PBS) (150 mM NaCl, 3.2 mM KCl, 6.4 mM Na_2HPO_4 12 H_2O, 1.5 mM KH_2PO_4, pH 7.4), and rinsed 6 times with Tris (Tris(hydroxymethyl)aminomethane hydrochloride) buffered saline (TBS) buffer (1 mM $CaCl_2$, 1 mM $MgCl_2$, 50 mM Tris–HCl, 150 mM NaCl, 10 mM Hepes (4-(2-Hydroxyethyl)piperazine-1-ethanesulfonic acid), pH 7.4). The cells were then incubated for 3 h at 37 °C with the contrast agents (4 μmol iron/mL corresponding to 0.364 nmol particles/mL; 1.5 nmol FN/mL and 1.02 nmol GRGD/mL, or a range of concentrations when mentioned) diluted in 200 μl TBS; the parent USPIO was used as a control. After rinsing 4 times with TBS, the contrast agents bound to the cells were digested with 100 μl 5 N HCl (24 h, 37 °C). The samples were analyzed by MRI with a T_2-weighted spin-echo sequence (Bruker AVANCE-200 system, 4.7 T, TR/TE = 3000/20-2000 ms, matrix $= 256 \times 256$, FOV = 5 cm, slice thickness = 2 mm), and the paramagnetic T_2 values of the acidic digested samples were measured on images. The Fe concentration was determined in each sample by using a calibration curve obtained from the MRI measurement of relaxation rate (ΔR_2) as a function of iron concentration (from 0.05 mM to 1.5 mM, digested in acidic solution); ΔR_2 is defined as $R_2^{obs} - R_2^{H_2O}$, where R_2^{obs} is the observed R_2. The measurements performed by MRI were compared each time by spectrophotometry with Prussian blue [37]. Finally, the results were used to estimate the apparent dissociation constants (K_d^*) of USPIO-g-FN, USPIO-g-GRGD and of USPIO-g-mimRGD for integrins expressed by Jurkat cells.

We have to point out that acidic digestion of the samples is necessary to re-suspend the contrast agents bound to the cells. The acidic digestion disintegrates the USPIO particles, which means that the final solution contains free iron ions. As a consequence, the assay is based on paramagnetic iron relaxivity, not on the superparamagnetic effect of USPIO particles. The iron concentration in an aqueous solution can be estimated by the measurement of both transverse or longitudinal relaxation rates because their relationship with iron concentration is described by a linear function. The transverse relaxivity of the paramagnetic iron ions is slightly higher than its longitudinal relaxivity [38]. Since the diamagnetic dilution medium after digestion is nearly water, its transverse and longitudinal relaxivities are roughly equal. Therefore, the determination of iron concentration based on one of the two parameters has roughly the same sensibility. The conclusion should be different in biological media because their transverse relaxivity is about 10 times higher than the longitudinal one. We have chosen to measure the transverse relaxation times by using a multi-echoes imaging sequence because it allows an easy, fast and accurate determination of the relaxation rate.

2.6. Competition with the free peptide in solution

The specific interaction of USPIO-g-FN, USPIO-g-GRGD and of USPIO-g-mimRGD with integrins was assessed by pre-incubating Jurkat cells, stimulated with PMA, with a range of concentrations of the corresponding peptide for 1 h, at 37 °C: 1.5–0.375 mg/mL for the CS1 fragment of fibronectin; 0.25–0.0625 mg/mL for GRGD in competition with USPIO-g-GRGD; 0.125–0.008 mg/mL for GRGD in competition with USPIO-g-mimRGD. Subsequently, the contrast agent was added at a concentration of 4 μmol iron/mL and the incubation continued for one additional hour. At the end, the protocol of C-MALISA was performed as previously described. The iron concentration in each sample was determined by Prussian blue reaction after the MRI session.

3. Results and discussion

To validate the C-MALISA technique, we have performed the following groups of experiments with the aim to: (1) identify the optimal concentration of the contrast agent to distinguish the activated from non-activated integrins; (2) validate the MRI measurements of iron concentration bound on cells; (3) determine the apparent dissociation constants of the contrast agents for integrins expressed on Jurkat cells; (4) prove the specificity of the contrast agents for integrins; (5) validate the potential of C-MALISA as an in vitro method of diagnosis.

3.1. The optimal concentration of contrast agent, validation of MRI measurement of iron concentration, and estimation of the apparent dissociation constants for integrins

Jurkat cells, stimulated or not with PMA, were incubated with various concentrations (0.125–4 μmol iron/mL, corresponding to 0.0117–0.364 nmol particles/mL) of USPIO-g-FN or USPIO-g-GRGD with the aim to identify the optimal concentration allowing the distinction between the activated and non-activated integrins. Fig. 2 shows the MR images of Jurkat cells incubated with USPIO-g-FN and digested. They reveal a striking difference between the stimulated cells and the non-stimulated ones. This difference is remarkable for the cells incubated with 4 μmol iron/mL and proves the specificity of this interaction.

The ΔR_2 measured on each image was converted in values of iron concentration based on the calibration curve shown in Figs. 3(a) and (b), and the results were compared with those obtained by spectrophotometry (Fig. 4). We can observe that there is a very good agreement between the iron concentrations obtained by both methods, confirming that, as expected, MRI can be confidently used to quantify the concentration of bound ligand.

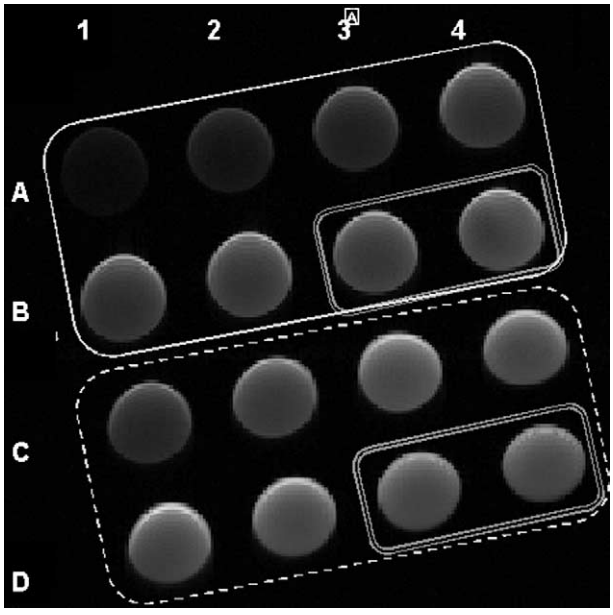

Fig. 2. The MR image (TR/TE = 3000/140 ms) of Jurkat cells stimulated (rows A and B) or not (rows C and D) with PMA and incubated with different concentrations (4–0.125 μmol iron/mL) of USPIO-g-FN: A1, C1 = 4 μmol iron/mL, A2, C2 = 2 μmol iron/mL, A3, C3 = 1 μmol iron/mL, A4, C4 = 0.5 μmol iron/mL, B1, D1 = 0.25 μmol iron/mL, B2, D2 = 0.125 μmol iron/mL. The samples included in double frames are the references. The images were acquired after acidic digestion of the samples in the presence of 5 N HCl as described in Section 2.

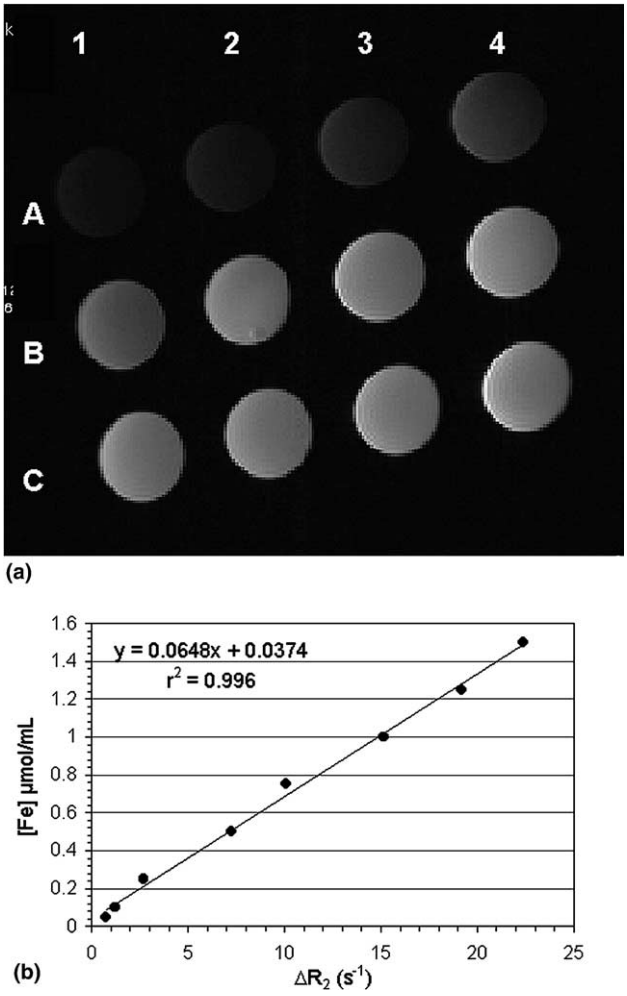

Fig. 3. Calibration curve for the estimation of the iron concentration in an acidic solution of 5 N HCl: (a) the MR image of a range of samples with different concentrations of iron; (b) the paramagnetic relaxation rates (ΔR_2) as a function of iron concentration measured by MRI. The ΔR_2 shown in (b) represents the averages of four calibration curves measured independently. The calibration curve contains the following concentrations of iron (μmol/mL): A1 = 1.5, A2 = 1.25, A3 = 1.0, A4 = 0.75, B1 = 0.50, B2 = 0.25, B3 = 0.10, B4 = 0.05. C1 and C2 contain 5 N HCl, C3 and C4 contain TBS.

Subsequently, we have tried to estimate the apparent dissociation constants (K_d^*) of the three contrast agents specific for integrins (Figs. 5(a)–(c)). For this purpose, their concentrations were converted to moles of particles/L by considering an average of 11,000 iron atoms per particle as explained in Section 2.

From Fig. 5, a K_d^* of 1.22×10^{-7} M, of 7.00×10^{-8} M, and of 1.13×10^{-8} M can be found for USPIO-g-FN, for USPIO-g-GRGD, and for USPIO-g-mimRGD, respectively. In the non-activated state, the K_d^* are of 1.81×10^{-7} M, of 9.32×10^{-7} M, and of 4.60×10^{-7} M. The K_d of the interaction between VCAM-1 (vascular cell adhesion molecule-1) and $\alpha_4\beta_1$ integrin ranges between 1.0×10^{-8} M and 1.0×10^{-7} M depending on the

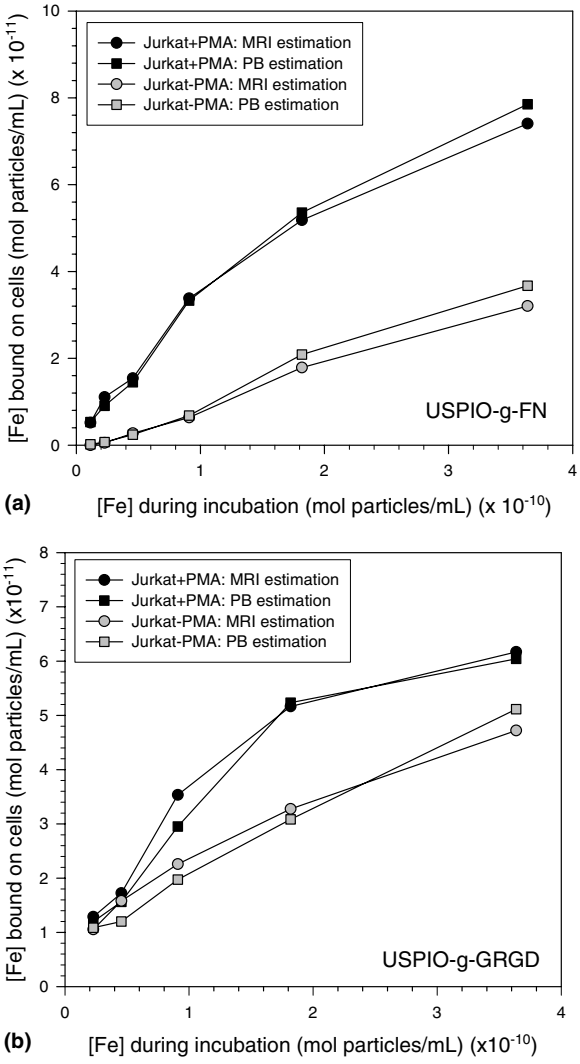

Fig. 4. Comparison between the iron concentration determined by MRI and by Prussian blue (PB) (see Section 2 for details) in samples of Jurkat cells stimulated or not with PMA and incubated with different concentrations (4–0.125 μmol iron/mL) of USPIO-g-FN (a) and USPIO-g-GRGD (b).

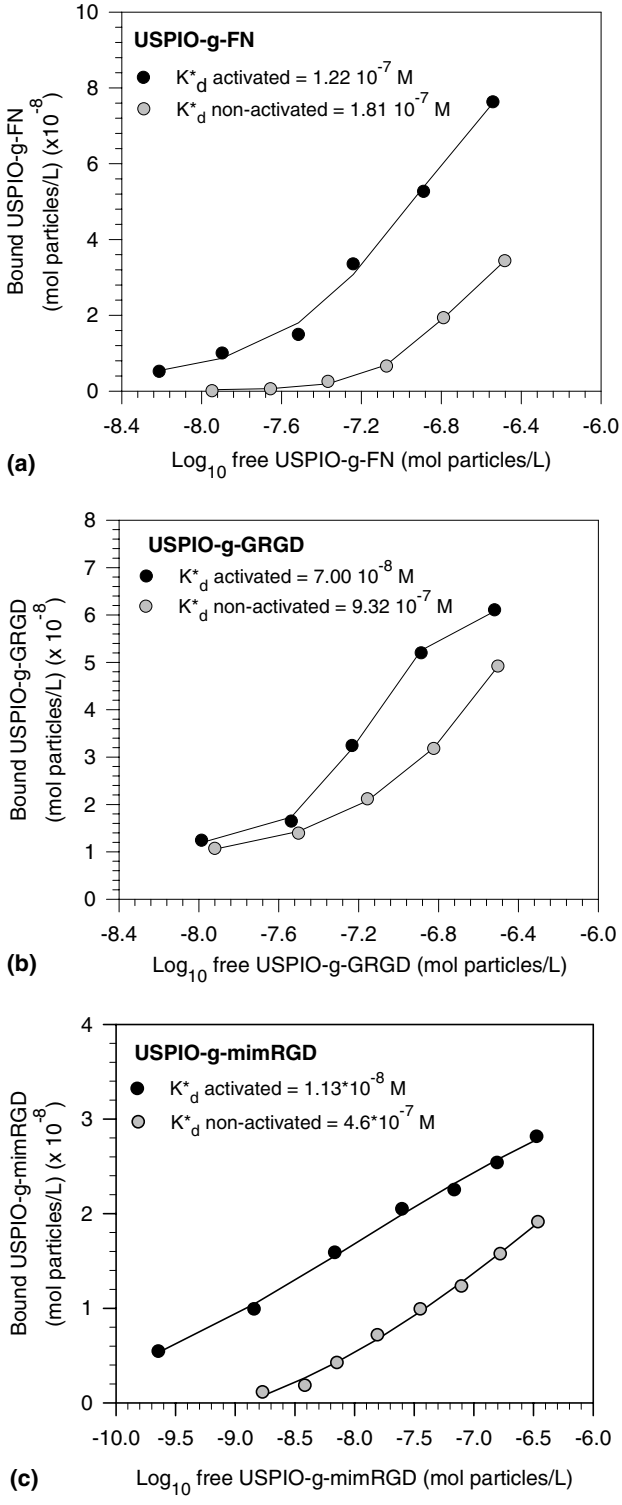

Fig. 5. The apparent dissociation constants (K_d^*) of USPIO-g-FN (a), of USPIO-g-GRGD (b), and of USPIO-g-mimRGD (c) for the integrins expressed on the surface of Jurkat cells in activated state and non-activated.

assaying conditions [39]. The K_d of an LDV motif containing peptide ranges between 3.0×10^{-10} M (in the presence of Mn^{2+}) and 1.2×10^{-8} M (in the absence of Mn^{2+}) [40]. In fact, integrins require extracellular divalent cations for ligand binding ability, and a concentration of 2 mM Mn^{2+} is capable of inducing/stabilizing ligand binding conformation [41]. In our experiments, Mn^{2+} could not be used to stabilize the interaction between contrast agents and the integrin-expressing Jurkat cells because this paramagnetic ion would affect the MRI signal intensity. This could probably explain the relatively lower affinities found in our study. On the other hand, the decreased affinity of the ligand after its grafting on a magnetic center is not unusual and has already been observed in literature for the Gal80-binding peptide conjugated to gadolinium-tetraazacyclododecanetetraacetic acid (Gd-DOTA) (Gd^{3+}-G80BP) [28].

3.2. Validation of the specific interaction of contrast agents with integrins

To assess the specific interaction of the three contrast agents with integrins, the cells were pre-incubated with the corresponding peptide (i.e., FN or GRGD) with the aim to inhibit the specific interaction of the contrast agents at the receptor sites.

The measurement of iron concentration (Fig. 6) proved that pre-incubation with non-grafted peptides diminished the concentration of bound contrast agents by 30–34% for USPIO-g-FN, by 84–87% for USPIO-g-GRGD, and by 66–70% for USPIO-g-mimRGD depending on the peptide concentration (Figs. 6(a)–(c)). This experiment confirms that our contrast agents interact specifically with integrins.

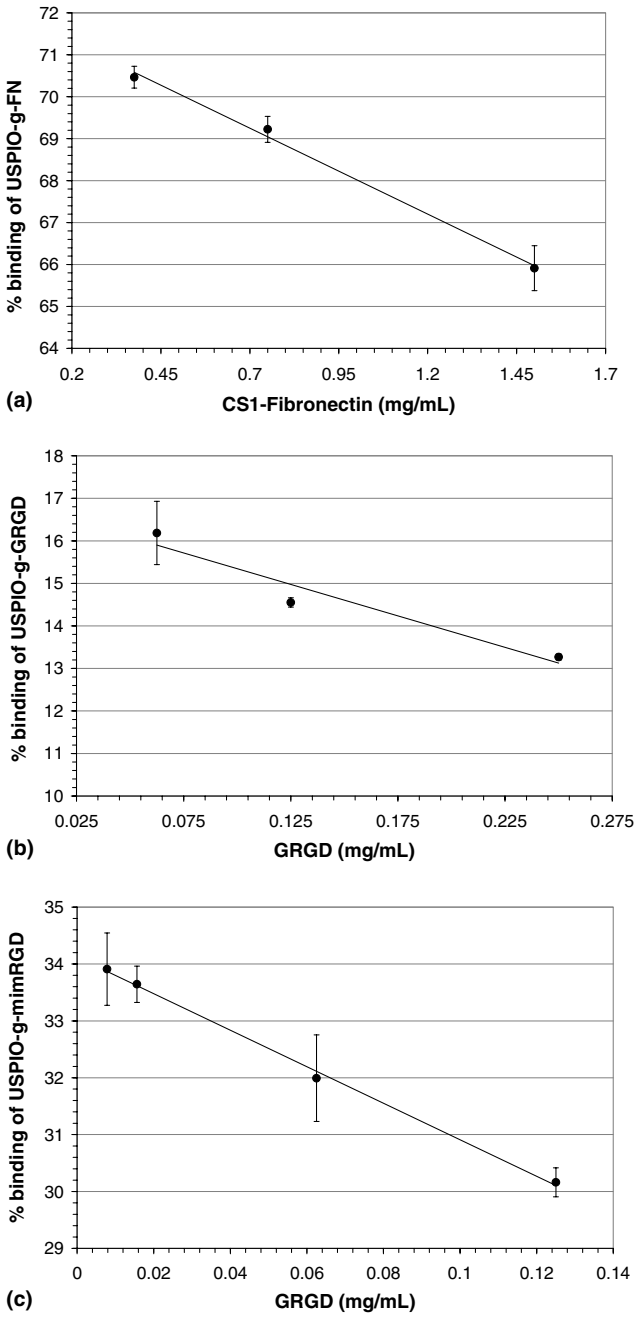

Fig. 6. Competition of USPIO-g-FN with CS1 fragment of fibronectin (FN) (a), and of USPIO-g-GRGD (b) and USPIO-g-mimRGD (c) with GRGD. The results are calculated as percentages of bound contrast agents after the pre-incubation with the competing peptides, which are FN for USPIO-g-FN (1.5, 0.75, 0.375 mg FN/mL), and GRGD for USPIO-g-GRGD (0.25, 0.125, 0.0625 mg GRGD/mL) and USPIO-g-mimRGD (0.125, 0.0625, 0.0156, 0.0078 GRGD mg/mL). The data represent averages of three experiments ± standard error of the mean.

3.3. Validation of C-MALISA as a clinical method of diagnosis

The efficiency of C-MALISA as an in vitro MRI method of diagnosis has been tested on MNC collected from Wistar rats with hepatitis induced by ConA and compared with the results obtained on Jurkat cells stimulated with PMA. The cells were incubated with the integrin-targeted contrast agents and the results were compared with the control samples (i.e., non-stimulated cells, cells incubated with USPIO).

The MRI (not shown) has indicated a significantly lower signal intensity of MNC activated with ConA or Jurkat cells stimulated with PMA and incubated with integrin-targeted compounds as compared to the control ones. These images suggested a specific interaction of integrin-targeted contrast agents with their receptors.

The ΔR_2 measured on each image was converted in values of iron concentration, which are presented in Fig. 7. The significant difference ($p < 0.01$ for USPIO-g-FN and USPIO-g-GRGD; $p < 0.05$ for USPIO-g-mimRGD) between the PMA- or ConA-stimulated cells and the non-activated ones supports the diagnostic potential of C-MALISA. The specific interaction of functionalized USPIO particles (USPIO-g-FN, USPIO-g-GRGD, and USPIO-g-mimRGD) with integrins is confirmed by the significant difference ($p < 0.01$) between the specific contrast agents and the non-specific one (USPIO).

4. Concluding remarks

The targeting of integrins with RGD containing molecules has extensively been explored for therapeutic [30] or diagnostic [14,15] purposes. In our work, the integrin targeting has been performed either with RGD motif (USPIO-g-GRGD) or with CS1 fragment of fibronectin (USPIO-g-FN) with the aim to develop an in vitro MRI method for clinical diagnosis. In addition, a new MRI strategy to target integrins has been attempted by grafting a non-peptide small molecular weight RGD mimetic [30] (USPIO-g-mimRGD) on USPIO particles. The effi-

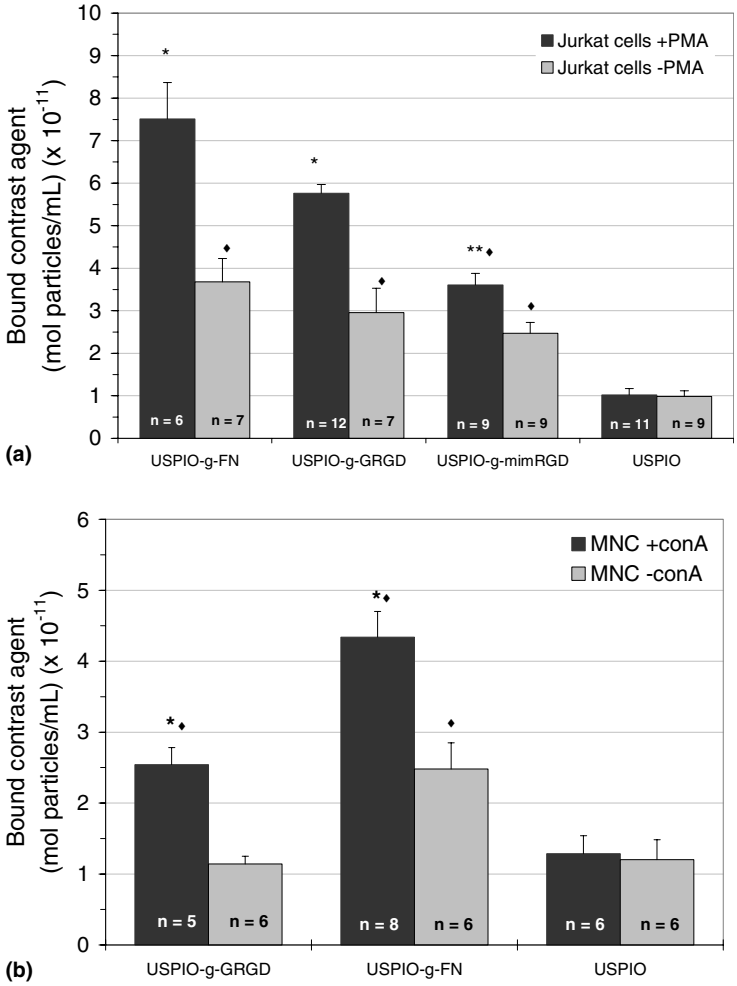

Fig. 7. Estimation of iron concentration bound on MNC (a) and on Jurkat cells (b) based on the ΔR_2 measured by MRI; the cells were incubated with 4 μmol iron/mL of contrast agent. The results are represented as averages ± standard error of the mean; the Student's t test has been calculated for each group versus cells non-stimulated with PMA (∗) or with ConA (∗) and versus USPIO (♦); ∗♦$p < 0.01$, ∗∗♦♦$p < 0.05$.

cacy of targeting to integrins of these homologous contrast agents, i.e., USPIO-g-GRGD, USPIO-g-FN and USPIO-g-mimRGD, has been tested in vitro on Jurkat cells and on rat MNC.

Various types of iron oxides have been developed recently and used as magnetic labels for targeted MR imaging due to their higher r_2 relaxivities as compared with paramagnetic labels. These properties facilitate the detection of cellular receptors at concentrations as low as 10^{-8} M [5,9]. A wide diversity of in vitro MR applications was proposed recently for magnetic nanoparticles, which demonstrate their potential in sensing different types of reversible molecular interactions, such as DNA–DNA, protein–protein, protein–small molecule, and enzyme reactions. Their detection was proposed to be run in a high-throughput, array-based format using MRI. All these studies confirmed that molecular interactions are associated with significant changes of T_2 or of the signal intensity, which enable the MR detection of the target molecule in concentrations as low as 53 fmol [27,29].

However, one of the crucial objectives in analytical biochemistry is to quantify the result of molecular interactions, which allows an accurate decision in diagnostic or pharmacological screening methodology. In our study, a new protocol was proposed to convert the MRI data in concentrations, which reflect the level of these interactions. C-MALISA can be performed in a high-throughput setting and it allows the accurate detection and quantification of the cell surface receptors. The procedure is fast, avoiding the steps of cell centrifugation, and permits the automatic running of the screening protocol. The direct labeling of the binding molecule (i.e., not by the intermediary of an enzyme-linked antibody) and the complete removal of the free ligand allows the real-time and real-state estimation of the kinetics of reactions. The applications are multiple and range from clinical diagnosis to

pharmacological screening of new drug targets and therapeutic molecules. In addition, the technique offers a second application for the contrast agents, which could be used for diagnostic purposes in vivo as well as in vitro.

In the actual version, the protocol of C-MALISA requires the acidic digestion of USPIO particles to reveal the compounds bound to the cell receptors. This procedure implies a diminished sensitivity towards the minimum concentration of receptors detectable by MRI because their estimation relies on the iron relaxivity and not on the relaxivity of USPIO particles, which is at least four times higher. An alternative to acidic digestion could be the destabilization of the ligand–receptor interaction either in the presence of a non-specific elution agent (e.g., glycine) or by treatment with a proteolytic enzyme. In this case, the protocol of C-MALISA could be performed in a shorter delay of time and its sensitivity could greatly be increased. Nevertheless, the method allows the estimation of bound receptors per cell since the value measured by MRI, i.e., ΔR_2, can be converted in number of particles and so in number of bound ligands. In our particular case, this estimation is not possible because of the large number and variety of integrin receptors expressed by leukocytes, which display a particular pattern in a signal- and time-dependent fashion [42].

We should also stress out that classical ELISA is a diagnostic technique that is already very well implemented in the clinical laboratory. As compared to this, C-MALISA in the actual context of the technical facility of the clinical laboratory is dependent on the MRI equipment, which is very expensive and not always accessible for a routine application. Though, the MRI device offers an advantage over ELISA plate readers because it enables the simultaneous assay of a large number of microtiter plates. The routine implementation of C-MALISA is furthermore sustained by the fact that many hospitals are already equipped with an MRI facility, while the use of magnetically labeled compounds could be more economical as compared to the battery of expensive ELISA-dedicated compounds. In this way, the specifically targeted compounds could be used for diagnostic purposes first in vitro on blood or biopsy specimens, and only after the expression of the targeted receptor was confirmed, the contrast agent could be used to confirm the pathology in vivo. Additionally, the large interest in the development of new magnetic-based immunoassay techniques will soon trigger the expansion of adequate high throughput screening equipment that is already under investigation [43–45]. Beside the clinical interest in these new magnetic-based devises, the ongoing field of molecular imaging requires the development of new techniques able to evaluate accurately the affinity constants of the new specifically targeted contrast agents.

Acknowledgments

The authors thank Mrs. Patricia de Francisco for her help in preparing the manuscript. This work was financially supported by the ARC program of the French Community of Belgium (research contract no. 00-05/258) and by the DGTRE (Region of Wallonia, NOMADE project).

References

[1] R.B. Lauffer, W.L. Greif, D.D. Stark, A.C. Vincent, S. Saini, V.J. Wedeen, T.J. Brady, J. Comput. Assist. Tomogr. 9 (3) (1985) 431–438.
[2] R. Weissleder, A.S. Lee, B.A. Khaw, T. Shen, T.J. Brady, Radiology 182 (1992) 381–385.
[3] H.-J. Weinmann, E. Wolfgang, B. Misselwitz, B. Schmitt, H. Schmitt-Willich, Eur. J. Radiol. 46 (2003) 33–44.
[4] T.J. Meade, A.K. Taylor, S.R. Bull, Curr. Opin. Neurobiol. 13 (2003) 597–602.
[5] H. Gupta, R. Weissleder, Magn. Reson. Imaging Clin. N. Am. 4 (1) (1996) 171–184.
[6] T. Shen, R. Weissleder, M. Papisov, A. Bogdanov Jr., T.J. Brady, Magn. Res. Med. 29 (1993) 599–604.
[7] L.H. Bryant, M.W. Brechbiel, C. Wu, J.W.M. Bulte, V. Herynek, J.A. Frank, J. Magn. Reson. Imaging 9 (1999) 348–352.
[8] P.M. Winter, A.M. Morawski, S.D. Caruthers, R.W. Fuhrhop, H. Zhang, T.A. Williams, J.S. Allen, E.K. Lacy, J.D. Robertson, G.M. Lanza, S.A. Wickline, Circulation 108 (2003) 2270–2274.
[9] A.D. Nunn, E. Linder, M.F. Tweedle, Q. J. Nucl. Med. 41 (2) (1997) 155–162.
[10] M. Rudin, R. Weissleder, Nat. Rev. Drug Discov. 2 (2003) 123–131.
[11] F.D. Rollo, Radiol. Manage. 25 (3) (2003) 28–32.
[12] J. Chen, C.-H. Tung, U. Mahmood, V. Ntziachristos, R. Gyurko, M.C. Fishman, P.L. Huang, R. Weissleder, Circulation 105 (2002) 2766–2771.
[13] X. Yu, S.-K. Song, J. Chen, M.J. Scott, R.J. Fuhrhop, C.S. Hall, P.J. Gaffney, S.A. Wickline, G.M. Lanza, Magn. Reson. Med. 44 (2000) 867–872.
[14] S.A. Anderson, R.K. Rader, W.F. Westlin, C. Null, G.M. Lanza, S.A. Wickline, J.J. Kotyk, Magn. Reson. Med. 44 (2000) 433–439.
[15] P.M. Winter, A.M. Morawski, S.D. Caruthers, R.W. Fuhrhop, H. Zhang, T.A. Williams, J.S. Allen, E.K. Lacy, J.D. Robertson, G.M. Lanza, S.A. Wickline, Circulation 108 (2003) 2270–2274.
[16] H.W. Kang, L. Josephson, A. Petrovsky, R. Weissleder, A. Bogdanov, Bioconjugate Chem. 13 (2002) 122–127.
[17] N.R. Sibson, A.M. Blamire, M. Bernades-Silva, S. Laurent, S. Boutry, R.N. Muller, P. Styles, D.C. Anthony, Magn. Reson. Med. 51 (2) (2004) 248–252.
[18] S. Boutry, C. Burtea, S. Laurent, L. Vander Elst, R.N. Muller, Magn. Reson. Med. 53(4) (2004) (in press).
[19] M. Zhao, D.A. Beauregard, L. Loizou, B. Davletov, M. Brindle, Nat. Med. 7 (11) (2001) 1241–1244.
[20] E.A. Schellenberger, D. Hogemann, L. Josephson, R. Weissleder, Acad. Radiol. 9 (2) (2002) S310–S311.
[21] C. Bremer, R. Weissleder, Acad. Radiol. 8 (2001) 15–23.
[22] T. Ichikawa, D. Högemann, Y. Saeki, E. Tyminski, K. Terada, R. Weissleder, E.A. Chiocca, J.P. Basilion, Neoplasia 4 (6) (2002) 523–530.
[23] J.W.M. Bulte, D.L. Kraitchman, NMR Biomed. 17 (2004) 484–499.

[24] D.D. Stark, R. Weissleder, G. Elizondo, P.F. Hahn, S. Saini, L.E. Todd, J. Wittenberg, J.T. Ferruci, Radiology 168 (1988) 297–301.
[25] S.G. Ruehm, C. Corot, P. Vogt, S. Kolb, J.F. Debatin, Circulation 103 (2001) 415–422.
[26] D.L. Kraitchman, A.W. Heldman, E. Atalar, L.C. Amado, B.J. Martin, M.F. Pittenger, J.M. Hare, J.W.M. Bulte, Circulation 107 (2003) 2290–2293.
[27] J.M. Perez, L. Josephson, T. O'Loughlin, D. Högemann, R. Weissleder, Nat. Biotechnol. 20 (2002) 816–820.
[28] L.M. De León-Rodriguez, A. Ortiz, A.L. Weiner, S. Zhang, Z. Kovacs, T. Kodadek, A.D. Sherry, J. Am. Chem. Soc. 124 (2002) 3514–3515.
[29] D. Högemann, V. Ntziachristos, L. Josephson, R. Weissleder, Bioconjugate Chem. 13 (2002) 116–121.
[30] G.A.G. Sulyok, C. Gibson, S.L. Goodman, G. Hölzemann, M. Wiesner, H. Kessler, J. Med. Chem. 44 (2001) 1938–1950.
[31] C. Pujades, R. Alon, R.L. Yauch, A. Masumoto, L.C. Burkly, C. Chen, T.A. Springer, R.R. Lobb, E. Hemler, Mol. Biol. Cell 8 (1997) 2647–2657.
[32] S. Johansson, G. Svineng, K. Wennerberg, A. Armulik, L. Lohikangas, Front. Biosci. 2 (1997) d126–d146.
[33] C. Gibson, S.L. Goodman, D. Hahn, G. Hoelzemann, H. Kessler, J. Org. Chem. 64 (1999) 7388–7394.
[34] L.L. Chen, A. Whitty, D. Scott, W.-C. Lee, M. Cornebise, S.P. Adams, R.C. Petter, R.R. Lobb, R.B. Pepinsky, J. Biol. Chem. 276 (39) (2001) 36520–36529.
[35] H. Morikawa, K. Hachiya, H. Mizuhara, Hepatology 31 (1) (2000) 83–94.
[36] K.W. Walker, R. Llull, G.K. Balkian, H.S. Ko, K.M. Flores, R. Ramsamooj, K.S. Black, C.W. Hewitt, D.C. Martin, J. Immunol. Methods 154 (1992) 121–130.
[37] I. Raynal, P. Prigent, S. Peyramaure, A. Najid, C. Rebuzzi, C. Corot, Invest. Radiol. 39 (1) (2004) 56–63.
[38] S.H. Koenig, R.D. Brown, M. Spiller, Magn. Reson. Med. 4 (1987).
[39] C. Pujades, R. Alon, R.L. Yauch, A. Masumoto, L.C. Burkly, C. Chen, T.A. Springer, R.R. Lobb, E. Hemler, Mol. Biol. Cell 8 (1997) 2647–2657.
[40] A. Chigaev, A.M. Blenc, J.V. Braaten, N. Kumaraswamy, C.L. Kepley, R.P. Andrews, J.M. Oliver, B.S. Edwards, E.R. Prossnitz, R.S. Larson, L.A. Sklar, J. Biol. Chem. 276 (52) (2001) 48670–48678.
[41] S. Johansson, G. Svineng, K. Wennerberg, A. Armulik, L. Lohikangas, Front. Biosci. 2 (1997) d126–d146.
[42] E.S. Harris, T.M. McIntyre, S.M. Prescott, G.A. Zimmerman, J. Biol. Chem. 275 (2000) 23409–23412.
[43] K. Kriz, J. Gehrke, D. Kriz, Biosens. Bioelectron. 13 (1998) 817–823.
[44] J. Richardson, P. Hawkins, R. Luxton, Biosens. Bioelectron. 16 (2001) 898.
[45] J. Richardson, A. Hill, R. Luxton, P. Hawkins, Biosens. Bioelectron. 16 (2001) 1127–1132.